Supplemental Materials for

Thermal and thermoelectric properties of monolayer indium triphosphide (InP_3): a first-principles study

Tao Ouyang[a)], Enlai Jiang, Chao Tang[a)], Jin Li, Chaoyu He, and Jianxin Zhong

Hunan Key Laboratory for Micro-Nano Energy Materials and Device and School of Physics and Optoelectronics, Xiangtan University, Xiangtan 411105, Hunan, China

1. The formation energy of monolayer InP_3 and possible preparation approachs

We calculate the formation energy of InP_3 on the fundamental of reaction process InP + 2P ---> InP_3, and the results are presented in Table. SI. It can be found that the formation energy in this process is about 0.256 eV (64 meV/atom), which is far smaller than the criteria (1 eV) proposed by the referee. This indicates that the monolayer InP_3 could be synthesized through such reaction process in experiment. Meanwhile, it should be mentioned here that bulk InP_3 is natural pseudo-two-dimensional crystal, and possesses planar 2D networks of puckered arsenic-type honeycomb structures. The calculated exfoliation energy of bulk InP_3 is about 1.32 J/m^2 [1], which is on the same order of magnitude of that of graphite (about 0.32 $\mp$ 0.03 J/m^2). That is to say, analogous to graphene, the monolayer InP_3 could also be prepared from its bulk form by utilizing mechanical cleavage or liquid phase exfoliation approaches.

[a)]Authors to whom correspondence should be addressed. Electronic addresses: ouyangtao@xtu.edu.cn and tang_chao@xtu.edu.cn

Table SI. The energy of monolayer InP, P atom in black phosphorene, and monolayer InP_3.

Reaction process: InP+2P→InP_3				
	InP	2*P	InP_3	ΔE
Energy (eV)	-7.4583	-10.732	-17.9348	0.2555

2. Lagrangian multiplier method used in ShengBTE for enforcing the translational invariance constraint of anharmonic force constants

Owning to the fact that the system energy does not change when the system as whole is displaced, one have the sum rules for third-order IFCs:

$$\sum_k \Phi_{ijk}^{\alpha\beta\gamma} = 0 \tag{S1}$$

However the directly calculated force constants from *ab*-initio package do not exactly satisfy all the sum rules. Therefore, the IFCs have to be enforced by changing the calculated value slightly since the sum rules are crucial to obtain the correct scattering rates especially the low frequencies. These can be done by solving an optimization problem. The idea is to add a compensation d_i to each independent nonzero element ϕ_i, where i ranges from 1 to the total number of independent nonzero elements, such that the sum rule condition can be satisfied. In order to guarantee that the compensation is small, some additional constraints need to be considered. The ShengBTE code minimize the sum of the squares of the compensation for each independent nonzero element, and the enforcement of sum rules turns out to be a minimization of a quadratic polynomial subject to constraints, which can be easily done by using the Lagrangian multiplier method [2,3].

Since all the IFCs can be deduced from the independent elements, the sums can be written in terms of these elements as:

$$\sum_j A_{ij}\Phi_j = B_i \tag{S2}$$

where A_{ij} are integers in the case of a cubic system, and j ranges from 1 to the total number of independent sums. Since the sum rules have to be satisfied, the constraints on the compensation are:

$$g_i \equiv \sum_j A_{ij}\Phi_j + B_i = 0 \tag{S3}$$

The function to be minimized is:

$$f = \frac{1}{2}\sum_j d_j^2 \tag{S4}$$

After introducing the Lagrangian multiplier λ_i, the expression of d_i in terms of λ_i could be obtained from

$$\frac{\partial(f + \sum_i \lambda_i g_i)}{\partial d_j} = 0 \tag{S5}$$

from which it follows:

$$d_j = -\sum_j \lambda_i A_{ij} \tag{S6}$$

Substituting this relation into Eq. (S3), one have

$$\sum_j C_{ij}\lambda_i = B_i \tag{S7}$$

with $C_{ij} = \sum_m A_{im}A_{jm}$, λ_j can be obtained by solving the linear equation arrays, and d_j is further obtained by using Eq. (S6), When d_j is added to the independent IFC elements ϕ_i, the sum rules are completely satisfied and the compensations are minimized.

3. Self-consistent test of the Grüneisen parameters of monolayer InP_3

In order to verify the accuracy of the third-order anharmonic IFCs, we calculate the Grüneisen parameters (γ_λ) which reflect the anharmonicity of a material and can be obtained from the anharmonic 3rd IFCs. Owning to the lacking of experimental data of monolayer InP_3, we perform a self-consistent test via changing the interaction cutoff of 3rd IFCs as shown in Fig. S1. It can be seen that the Grüneisen parameters vary obviously for the anharmonic IFCs when the interaction cutoff is short. However, the Grüneisen parameters stay almost unchanged for the interaction cutoff larger than fourth nearest neighbors. That is to say, the Grüneisen parameters of InP_3 are convergent when the interaction cutoff of IFCs is larger than fourth nearest neighbors, which could qualitatively characterize the accuracy of anharmonic force constants. Taking the computational accuracy and time-consuming of calculation into consideration, the sixth nearest neighbors are chosen as the interaction cutoff for the third-order IFCs in the following works.

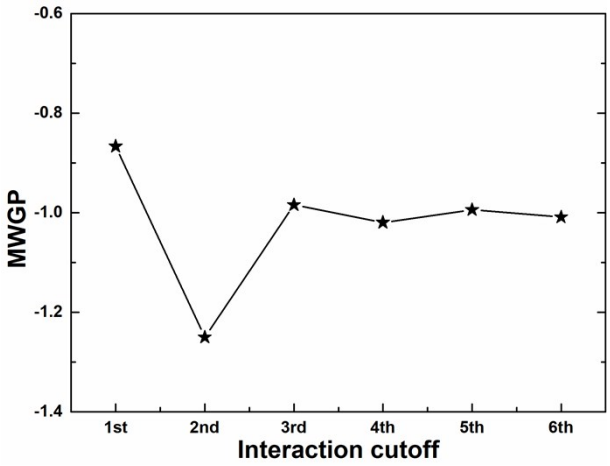

Fig. S1. The mode weighted accumulative Grüneisen parameter (MWGP) with respect to the interaction cutoff.

4. The thermal stability of monolayer InP_3

In this work, we mainly study the possibility of monolayer InP_3 in the field of recombination of photovoltaic and thermoelectric technologies together. Therefore, high temperature is not necessary under this circumstance. In order to demonstrate the thermal stability of monolayer InP_3, taken 500 K as an example, we perform *ab*-initio molecular dynamic (AIMD) simulations with $5 \times 5 \times 1$ supercell. From Fig. S2, one can find that after heating at 500 K for 10.0 ps with a time step of 1.0 fs, the puckered arsenic-type honeycomb networks are well maintained, and all the atoms in monolayer InP_3 cell are vibrating around their equilibrium positions during the simulations. The thermal stability of monolayer InP_3 could be further confirmed by the time-dependent evolution of total energies, which are oscillating within a very narrow range. Such results indicate that monolayer InP_3 is suitable for thermoelectric applications with medium temperature zone (around 500 K) and a promising candidate for achieving the recombination of photovoltaic and thermoelectric technologies together.

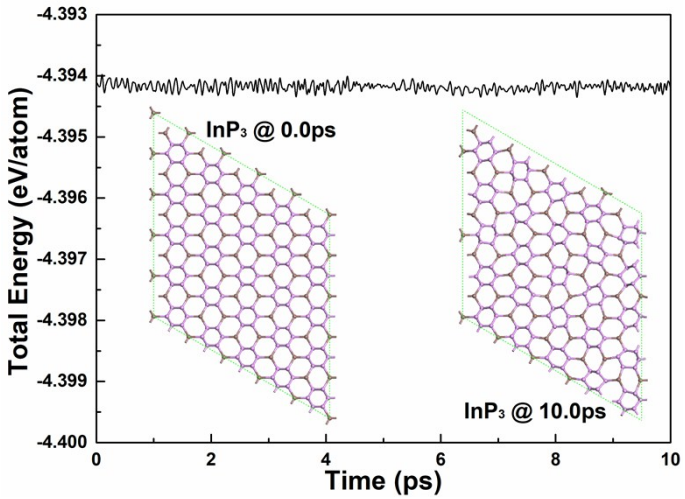

Fig. S2. The evolution of total energy and snapshots of monolayer InP3 from AIMD simulations at 500 K.

5. The doping effect on the electronic and phononic properties of monolayer InP_3

Based on the rigid band approximation of Boltzmann theory, the low concentration (smaller than 0.001 per atom) of monolayer InP_3 will only shift the Fermi-level and play a weak influence on the electronic structure. It should be noted that this approximation is reasonable as doping concentration is low, and has been utilized extensively for theoretical study of thermoelectric materials [4-9]. As for the doping effect on the phonon transport properties, the dopants will introduce impurity phonon scattering in addition to the intrinsic phonon-phonon scattering. The impurity phonon scattering can be considered through incorporating a Reyleigh-type term [10], ${\tau_{imp}}^{-1} = A\omega^4$ ($A = \left(3V_0^2S^2\right)N_{imp}/\pi v^3$), where V_0 is the volume of the unit cell, v the group velocity of phonon, N_{imp} the impurity concentration and S denotes the scattering factor setting as unity here. This scattering term can be added to the intrinsic phonon-phonon relaxation time by using the Matthiessen rule [11], ${\tau_{tot}}^{-1} = {\tau_{int}}^{-1} + {\tau_{imp}}^{-1}$, where τ_{tot} is the total phonon relaxation time, τ_{int} and τ_{imp} are the relaxation time induced by the intrinsic phonon-phonon scattering and

impurity phonon scattering, respectively. As one can note from Fig. S3(a) that the calculated lattice thermal conductivity of monolayer InP3 decreases after impurity phonon scattering are considered. However, the effect of such slight reduction of lattice thermal conductivity on the thermoelectric figure of merit is quite limited, as shown in Fig. S3(b). This because that the figure of merit depends on not only the lattice thermal conductivity but also electronic thermal conductivity.

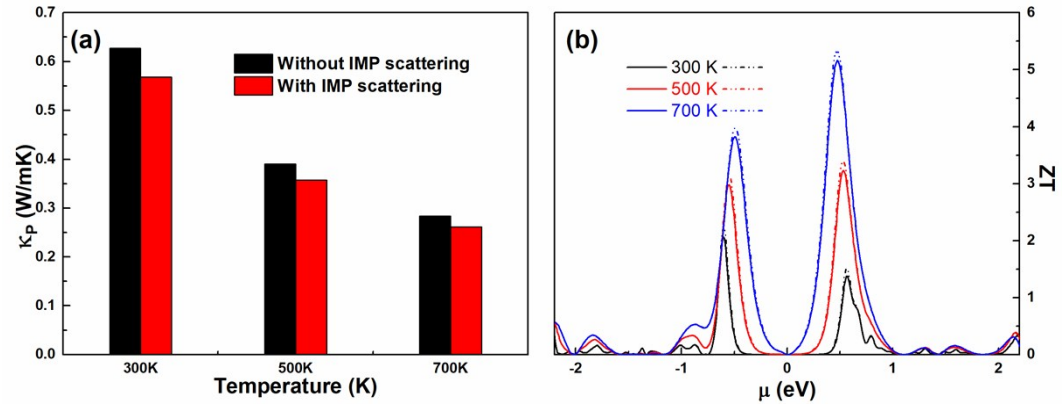

Fig. R2. (a) The average lattice thermal conductivity of monolayer InP_3 with and without considering impurity phonon scattering. (b) The thermoelectric figure of merit (*ZT*) as a function of chemical potential of monolayer InP_3 along armchair directions. The doted-dashed (solid) line represents the results based on lattice thermal conductivity with (without) impurity phonon scattering.

6. The effect of relaxation time of the thermoelectric performance of monolayer InP_3

The electron relaxation time might exist a little difference when electron locates in the band edges or within the bands. However, it is quite difficult to calculate the relaxation time within the valence or conduction bands from the first-principle calculations. Therefore, in this work we utilize the electron relaxation time in the band edges to estimate the thermoelectric performance of monolayer InP_3, which is also a common treatment in previous first principles thermoelectric calculations [4-9]. In order to investigate such influence on thermoelectric performance, we

recalculate the room temperature figure of merit (ZT) of InP_3 with different electron relaxation time. From Fig. S4 one can note that although the relaxation time is reduced by half, the thermoelectric figure of merit ZT of monolayer InP_3 could still approach 1.51 (with p-type doping) and 0.44 (with n-type doping) along armchair and zigzag directions. This result further demonstrates that monolayer InP_3 is a competitive thermoelectric material.

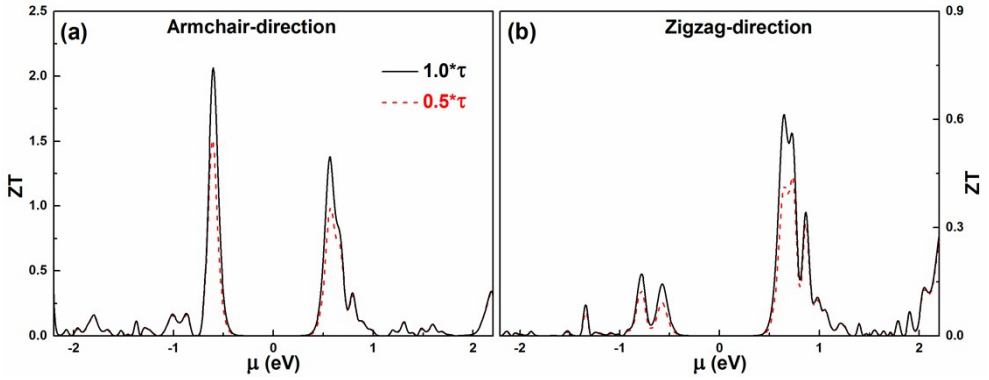

Fig. S4. The room temperature thermoelectric figure of merit (ZT) as a function of chemical potential of monolayer InP_3 along (a) armchair and (b) zigzag directions with different electron relaxation time τ. The electron relaxation time τ is estimated from the deformation potential theory [1].

References

[1] N. Miao, B. Xu, N. C. Bristowe, J. Zhou and Z. Sun, J. Am. Chem. Soc., 2017, 139, 11125-11131.
[2] W. Li, L. Lindsay, D. A. Broido, D. A. Stewart and N. Mingo, Phys. Rev. B, 2012, 86, 174307.
[3] N. Mingo, D. A. Stewart, D. A. Broido and D. Srivastava, Phys. Rev. B, 2008, 77, 033418.
[4] D. J. Singh, Physical Review B, 2007, 76, 085110.
[5] D. Parker and D. J. Singh, Phys. Rev. X, 2011, 1, 021005.
[6] G. K. H. Madsen, J. Am. Chem. Soc., 2006, 128, 12140-12146.
[7] J. F. Sun and D. J. Singh, J. Mater. Chem. A, 5, 8499 (2017).
[8] Y. W. Li, D. J. Singh, M. H. Du, Q. L. Xu, L. J. Zhang, W. T. Zheng, and Y. M. Ma, J. Mater. Chem. C, 4, 4592 (2016).
[9] L. Xi, Y. B. Zhang, X. Y. Shi, J. Yang, X. Shi, L. D. Chen, W. Zhang, Jihui Yang, and D. J. Singh, Phys. Rev. B, 86, 155201 (2012).
[10] P. G. Klemens, Proc. Phys. Soc., London, Sect. A 68, 1113 (1955).
[11] T. Feng and X. Ruan, J. Nanomater. 2014, 206370 (2014).